ICSV13 - Vienna
The Thirteenth International Congress on Sound and Vibration
Vienna, Austria, July 2-6, 2006

VIBRATIONS OF NONLINEAR STRUCTURES USING STRUCTURAL COUPLING METHOD

Dae-Kwan Kim[1], and Jae-Hung Han*[1]

[1]Division of Aerospace Engineering, Korea Advanced Institute of Science and Technology
373-1 Guseong-dong, Yuseong-gu, Daejeon, 305-701, Korea
jaehunghan@kaist.ac.k

Abstract
A structural coupling method is developed for the dynamic analysis of a nonlinear structure, consisting of substructures and concentrated nonlinear hinge joints or sliding lines. Component mode synthesis method is extended to couple the substructures and the nonlinear interfaces, so that iterative problems such as flutter analysis can be efficiently analyzed with a reasonable cost and time. In order to verify the improved coupling method, a numerical plate model consisting of two substructures and torsional springs, is synthesized by using the proposed method and its model parameters are compared with analysis data. Then the coupling method is applied to a three-substructure-model with the nonlinearity of sliding lines between the substructures. The coupled structural model is verified from its dynamic analysis. The analysis results show that the improved coupling method is adequate for the nonlinear structural analyses with as the nonlinear hinge and sliding mode condition.

INTRODUCTION

Most practical engineering structures are complicated with have some structural nonlinearities. As an example, a deployable missile control fin has a nonlinear hinge joint which consists of a torsional spring, a compression spring and several stoppers. Because of wear and manufacturing tolerance, the hinge has some structural nonlinearities such as preload, free-play, asymmetric bilinear stiffness, hysterisis and coulomb damping. Another example can be a pantograph tilting structure consisting of a pantograph, sledge and base frames. There is a structural nonlinearity of sliding lines between the base frame and the sledge, which is restricted to follow guide lines on the base frame. These nonlinearities are impossible to be completely eliminated, and exert significant effects on the static and dynamic characteristics. Therefore, it is necessary to establish an accurate structural dynamic model to predict or control the nonlinear dynamic systems. However, it is very difficult to directly apply full order nonlinear finite element models to many practical engineering problems, especially when iterate analyses are required as in the time-domain nonlinear flutter analysis [1].

In general, the information about the position of a structural nonlinearity offers opportunities to separate the total structure into linear and nonlinear components so that they can be separately analyzed. Substructure synthesis method is a structural coupling method for combining the substructures represented with reduced degrees of freedom (DOF). There have been many studies on the substructure synthesis method [4, 5]. Hunn introduced the first partial modal coupling method [3]. Craig and Bampton treated the displacements of substructures as being composed of constraint modes and normal modes [2]. Kim et al. extended Craig-Bampton method to consider concentrated structural nonlinearities and then applied the improved method to a deployable missile control fin [6].

In the present study, the Craig-Bampton method is improved to consider not only the concentrated structural nonlinearities but also the sliding mode condition. In order to validate the improved coupling method, a numerical plate model consisting of two substructures and seven torsional springs is synthesized by using the improved method, and its model parameters are compared with analysis data. Then, the coupling method is applied to a three-substructure-model with the structural nonlinearity of sliding lines between the substructures, and the coupled structural model is verified with dynamic results.

SUBSTRUCTURE SYNTHESIS FOR HINGE JOINTS

The substructure synthesis method, [2] extended to consider concentrated nonlinear hinge joints, is summarized in this section. In order to verify the method, a numerical plate model with two substructures and seven torsional springs is synthesized by using the improved method, and its model parameters are compared with analysis data.

Extended Substructure Synthesis Method

To analyze the dynamic characteristics of a complex structure by using the substructure synthesis method, it is necessary to divide the whole structure into a limited number of substructures. Each substructure is connected to at least one of other substructures as shown in figure 1.

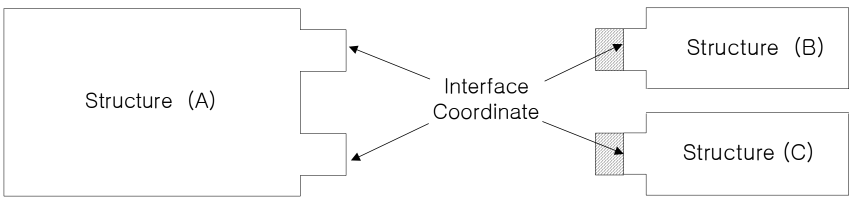

Figure 1 – A scheme of separate structure analysis

For an arbitrary linear undamped substructure, the generalized equations of motion of Sub-A are written as

$$\begin{bmatrix} m_{RR}^{(A)} & m_{RI}^{(A)} \\ m_{RI}^{(A)T} & m_{II}^{(A)} \end{bmatrix} \begin{Bmatrix} \ddot{\xi}_R^{(A)} \\ \ddot{\xi}_I^{(A)} \end{Bmatrix} + \begin{bmatrix} \omega_R^{2(A)} & 0 \\ 0 & k_I^{(A)} \end{bmatrix} \begin{Bmatrix} \xi_R^{(A)} \\ \xi_I^{(A)} \end{Bmatrix} = \begin{Bmatrix} 0 \\ F_I^{(A)} \end{Bmatrix} \tag{1}$$

where the generalized mass and stiffness matrices, and displacement and force vectors are partitioned according to the interior (R) and interface (I) coordinates of the substructure. The vector $\{F_I\}$ is the force vector applied at the interface coordinates by adjoining substructures.

For the simplicity of the problem, it is assumed that the whole structure consists of two substructures (Sub-A and Sub-B), and there are no external forces applied to the interior coordinates of the substructures. If the two substructures are coupled by torsional springs located at some of the interface coordinates, the interface coordinates of each substructure can be divided into the coordinates (I_p) with torsional springs and the other coordinates (I_n) [6]. The generalized equations of motion of Sub-A and Sub-B can be expressed as

$$\begin{bmatrix} m_{RR}^{(A)} & m_{RI_n}^{(A)} & m_{RI_p}^{(A)} \\ m_{RI_n}^{(A)T} & m_{I_nI_n}^{(A)} & m_{I_nI_p}^{(A)} \\ m_{RI_p}^{(A)T} & m_{I_nI_p}^{(A)\,T} & m_{I_pI_p}^{(A)} \end{bmatrix} \begin{Bmatrix} \ddot{\xi}_R^{(A)} \\ \ddot{\xi}_{I_n}^{(A)} \\ \ddot{\xi}_{I_p}^{(A)} \end{Bmatrix} + \begin{bmatrix} \omega_R^{2(A)} & 0 & 0 \\ 0 & k_{I_nI_n}^{(A)} & k_{I_nI_p}^{(A)} \\ 0 & k_{I_nI_p}^{(A)\,T} & k_{I_pI_p}^{(A)} \end{bmatrix} \begin{Bmatrix} \xi_R^{(A)} \\ \xi_{I_n}^{(A)} \\ \xi_{I_p}^{(A)} \end{Bmatrix} = \begin{Bmatrix} 0 \\ F_{I_n}^{(A)} \\ F_{I_p}^{(A)} \end{Bmatrix} \tag{2}$$

$$\begin{bmatrix} m_{I_nI_n}^{(B)} & m_{I_nI_p}^{(B)\,T} & m_{RI_n}^{(B)T} \\ m_{I_nI_p}^{(B)} & m_{I_pI_p}^{(B)} & m_{RI_p}^{(B)T} \\ m_{RI_n}^{(B)} & m_{RI_p}^{(B)} & m_{RR}^{(B)} \end{bmatrix} \begin{Bmatrix} \ddot{\xi}_{I_n}^{(B)} \\ \ddot{\xi}_{I_p}^{(B)} \\ \ddot{\xi}_R^{(B)} \end{Bmatrix} + \begin{bmatrix} k_{I_nI_n}^{(B)} & k_{I_nI_p}^{(B)} & 0 \\ k_{I_nI_p}^{(B)\,T} & k_{I_pI_p}^{(B)} & 0 \\ 0 & 0 & \omega_R^{2(B)} \end{bmatrix} \begin{Bmatrix} \xi_{I_n}^{(B)} \\ \xi_{I_p}^{(B)} \\ \xi_R^{(B)} \end{Bmatrix} = \begin{Bmatrix} F_{I_n}^{(B)} \\ F_{I_p}^{(B)} \\ 0 \end{Bmatrix} \tag{3}$$

The compatibility equations of the interface coordinates (I_p, I_n) of the two substructures can be written as follows:

$$\left\{u_{I_n}^{(A)}\right\} = \left\{u_{I_n}^{(B)}\right\} = \left\{u_{I_n}\right\},\ \left\{\xi_{I_n}^{(A)}\right\} = \left\{\xi_{I_n}^{(B)}\right\} = \left\{\xi_{I_n}\right\} \tag{4}$$

$$\left\{F_{I_p}^{(A)}\right\} = \left[K_\theta\right]\left(\left\{u_{I_p}^{(B)}\right\} - \left\{u_{I_p}^{(A)}\right\}\right) = \left[K_\theta\right]\left(\left\{\xi_{I_p}^{(B)}\right\} - \left\{\xi_{I_p}^{(A)}\right\}\right) \tag{5}$$

$$\left\{F_{I_p}^{(B)}\right\} = -\left[K_\theta\right]\left(\left\{u_{I_p}^{(B)}\right\} - \left\{u_{I_p}^{(A)}\right\}\right) = -\left[K_\theta\right]\left(\left\{\xi_{I_p}^{(B)}\right\} - \left\{\xi_{I_p}^{(A)}\right\}\right) \tag{6}$$

where $[K_\theta]$ is a diagonal matrix of the torsional spring coefficients according to each I_p. Substitution of Eqs. (4), (5) and (6) into Eqs. (2) and (3), and the coupling of these equations gives

$$
\begin{bmatrix}
m_{RR}^{(A)} & m_{RI_n}^{(A)} & m_{RI_p}^{(A)} & 0 & 0 \\
m_{RI_n}^{(A)T} & m_{I_nI_n}^{(A)}+m_{I_nI_n}^{(B)} & m_{I_nI_p}^{(A)} & m_{I_nI_p}^{(B)\,T} & m_{RI_n}^{(B)T} \\
m_{RI_p}^{(A)T} & m_{I_nI_p}^{(A)\,T} & m_{I_pI_p}^{(A)} & 0 & 0 \\
0 & m_{I_nI_p}^{(B)} & 0 & m_{I_pI_p}^{(B)} & m_{RI_p}^{(B)T} \\
0 & m_{RI_n}^{(B)} & 0 & m_{RI_p}^{(B)} & m_{RR}^{(B)}
\end{bmatrix}
\begin{Bmatrix}
\ddot{\xi}_R^{(A)} \\ \ddot{\xi}_{I_n} \\ \ddot{\xi}_{I_p}^{(A)} \\ \ddot{\xi}_{I_p}^{(B)} \\ \ddot{\xi}_R^{(B)}
\end{Bmatrix}
+
\begin{bmatrix}
\omega_R^{2(A)} & 0 & 0 & 0 & 0 \\
0 & k_{I_nI_n}^{(A)}+k_{I_nI_n}^{(B)} & k_{I_nI_p}^{(A)} & k_{I_nI_p}^{(B)} & 0 \\
0 & k_{I_nI_p}^{(A)\,T} & k_{I_pI_p}^{(A)}+K_\theta & -K_\theta & 0 \\
0 & k_{I_nI_p}^{(B)\,T} & -K_\theta & k_{I_pI_p}^{(B)}+K_\theta & 0 \\
0 & 0 & 0 & 0 & \omega_R^{2(B)}
\end{bmatrix}
\begin{Bmatrix}
\xi_R^{(A)} \\ \xi_{I_n} \\ \xi_{I_p}^{(A)} \\ \xi_{I_p}^{(B)} \\ \xi_R^{(B)}
\end{Bmatrix}
= \{0\} \tag{7}
$$

The natural frequencies and eigenvectors of the combined structure with torsional springs can be easily obtained from Eq. (7), which can be applied to the complex structure problems with several substructures.

Free Vibration Example

To verify the extended substructure synthesis method, the free vibration of a cantilever plate is considered. The plate has two substructures coupled by a hinge section with seven torsional springs as shown in figure 2. Each node has three DOFs, one translation and two rotations. The torsional spring coefficient, elastic modulus, density and Poisson ratio used for the example are $K_\theta = 1Nm/rad$, 72GPa, $2800kg/m^3$ and 0.33, respectively. The frequency range of interest is chosen to be 0Hz to 500Hz. The lowest one and seven normal modes are used to represent Sub-A and Sub-B, respectively.

The natural frequencies and mode shapes calculated by the present extended method are compared with those calculated by using MSC/NASTRAN®. Table 1 gives the modal parameter results. It is clear that the normal modes of the entire structure are accurately obtained by using the extended method.

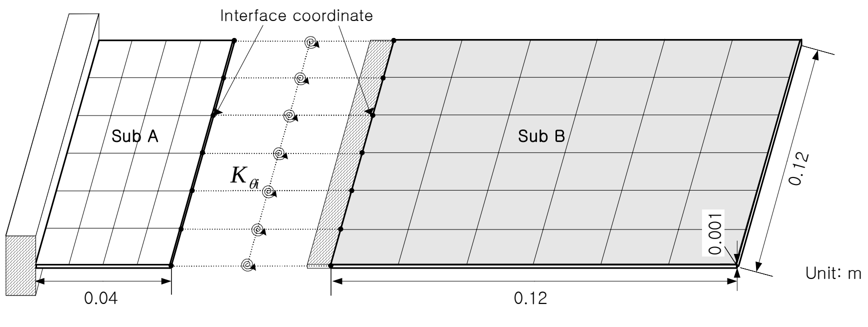

Figure 2 – A scheme of plate model with two components and torsional springs

Table 1 – Comparison of Natural frequency between NASTRAN and present method

Frequency(Hz), Error(%) and MAC									
Mode	Nastran	Present	Error	MAC	Mode	Nastran	Present	Error	MAC
1	22.26	22.26	0.000	1.000	5	418.12	418.37	0.059	1.000
2	99.42	99.43	0.004	1.000	6	508.51	509.46	0.188	1.000
3	207.38	207.41	0.016	1.000	7	665.90	679.08	1.979	0.981
4	343.55	344.90	0.392	0.998	8	703.20	708.77	0.792	0.994

SUBSTRUCTURE SYNTHESIS FOR SLIDING CONDITION

The extended substructure synthesis method described in the previous section is improved to consider the sliding mode condition. For the validation of the improved method, it is applied to a three-substructure-model with the structural nonlinearity of sliding lines between the substructures, and the dynamic analysis of the coupled structural model is performed for a sinusoidal external force.

Improved Substructure Synthesis Method

In order to consider the sliding mode condition, it is assumed that the whole structure consists of two substructures (Sub-A and Sub-B), and there is a sliding mode condition between the substructures as shown in figure 3. The interface coordinates of the Sub-A and Sub-B are the guide line and the roller, respectively, and the roller is restricted to follow the guide line.

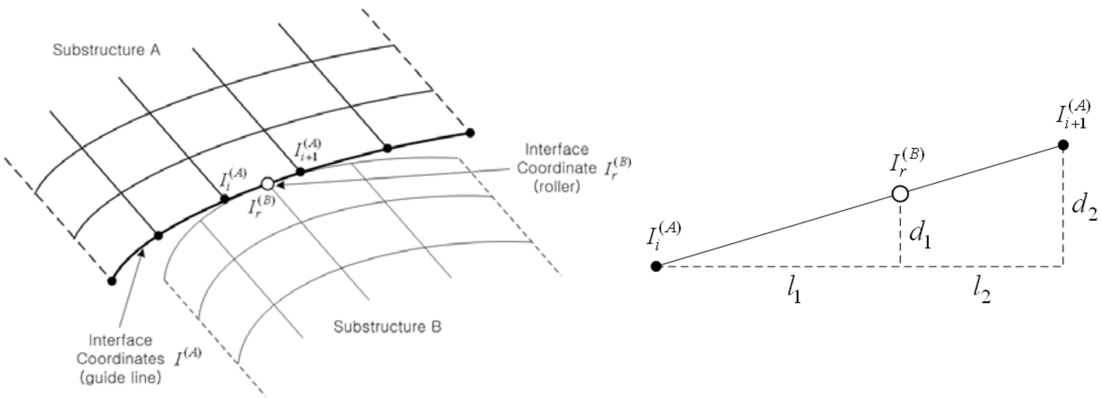

Figure 3 – A scheme of separate structure analysis with sliding mode condition

If the roller coordinate I_r is located between two coordinates, I_i and I_{i+1}, of the guide line, which are assumed to be continuous DOFs, then the generalized equations of motion of Sub-A and Sub-B can be expressed in the same manner of Eqs. (2) and (3) as follows:

$$\left[\begin{array}{c:c:c:c:c} m_{RR}^{(A)} & & m_{RI_i}^{(A)} & m_{RI_{i+1}}^{(A)} & \\ \hdashline & & & & \\ \hdashline m_{RI_i}^{(A)T} & & m_{I_iI_i}^{(A)} & m_{I_iI_{i+1}}^{(A)} & \\ \hdashline m_{RI_{i+1}}^{(A)T} & & m_{I_iI_{i+1}}^{(A)T} & m_{I_{i+1}I_{i+1}}^{(A)} & \\ \hdashline & & & & \end{array}\right]\left\{\begin{array}{c} \ddot{\xi}_R^{(A)} \\ \hdashline \vdots \\ \hdashline \ddot{\xi}_{I_i}^{(A)} \\ \hdashline \ddot{\xi}_{I_{i+1}}^{(A)} \\ \hdashline \vdots \end{array}\right\}+\left[\begin{array}{c:c:c:c:c} k_{RR}^{(A)} & & k_{RI_i}^{(A)} & k_{RI_{i+1}}^{(A)} & \\ \hdashline & & & & \\ \hdashline k_{RI_i}^{(A)T} & & k_{I_iI_i}^{(A)} & k_{I_iI_{i+1}}^{(A)} & \\ \hdashline k_{RI_{i+1}}^{(A)T} & & k_{I_iI_{i+1}}^{(A)T} & k_{I_{i+1}I_{i+1}}^{(A)} & \\ \hdashline & & & & \end{array}\right]\left\{\begin{array}{c} \xi_R^{(A)} \\ \hdashline \vdots \\ \hdashline \xi_{I_i}^{(A)} \\ \hdashline \xi_{I_{i+1}}^{(A)} \\ \hdashline \vdots \end{array}\right\}=\left\{\begin{array}{c} 0 \\ \hdashline 0 \\ \hdashline F_{I_i}^{(A)} \\ \hdashline F_{I_{i+1}}^{(A)} \\ \hdashline 0 \end{array}\right\} \tag{8}$$

$$\begin{bmatrix} m_{I_rI_r}^{(B)} & m_{RI_r}^{(B)} \\ m_{RI_r}^{(B)T} & m_{RR}^{(B)} \end{bmatrix}\begin{Bmatrix} \ddot{\xi}_{I_r}^{(B)} \\ \ddot{\xi}_R^{(B)} \end{Bmatrix}+\begin{bmatrix} k_{I_rI_r}^{(B)} & k_{RI_r}^{(B)} \\ k_{RI_r}^{(B)T} & k_{RR}^{(B)} \end{bmatrix}\begin{Bmatrix} \xi_{I_r}^{(B)} \\ \xi_R^{(B)} \end{Bmatrix}=\begin{Bmatrix} F_{I_r}^{(B)} \\ \bar{F}_R^{(B)} \end{Bmatrix} \tag{9}$$

where $\left\{\bar{F}_R^{(B)}\right\}=\left[\Psi_N^{(B)T}\right]\left\{F_R^{(B)}\right\}$ and $\left[\Psi_N^{(B)T}\right]$ is the normal mode of the Sub-B.

For the synthesis of the substructures, the compatibility equations of the interface coordinates (I_i, I_{i+1} and I_r) can be written as follows:

$$\left\{F_{I_i}^{(A)}\right\}=-\frac{l_2^A}{l_1^A+l_2^A}\left\{F_{I_r}^{(B)}\right\}=-c_i^A\left\{F_{I_r}^{(B)}\right\} \tag{10}$$

$$\left\{F_{I_{i+1}}^{(A)}\right\}=-\frac{l_1^A}{l_1^A+l_2^A}\left\{F_{I_r}^{(B)}\right\}=-c_{i+1}^A\left\{F_{I_r}^{(B)}\right\} \tag{11}$$

$$\left\{\xi_{I_r}^{(B)}\right\}=c_i^A\left\{\xi_{I_i}^{(A)}\right\}+c_{i+1}^A\left\{\xi_{I_{i+1}}^{(A)}\right\} \tag{12}$$

where l_1 and l_2 are the horizontal displacements between the interface coordinates and the roller as shown in figure 3. Substitution of Eqs. (10), (11) and (12) into Eqs. (8) and (9), and the coupling of these equations gives

$$\left[\begin{array}{c:c:c:c:c:c} m_{RR}^{(A)} & & m_{RI_i}^{(A)} & m_{RI_{i+1}}^{(A)} & & 0 \\ \hdashline & & & & & 0 \\ \hdashline m_{RI_i}^{(A)T} & & m_{I_iI_i}^{(A)}+c_i^Ac_i^Am_{I_rI_r}^{(B)} & m_{I_iI_{i+1}}^{(A)}+c_i^Ac_{i+1}^Am_{I_rI_r}^{(B)} & & c_i^Am_{RI_r}^{(B)} \\ \hdashline m_{RI_{i+1}}^{(A)T} & & m_{I_iI_{i+1}}^{(A)T}+c_i^Ac_{i+1}^Am_{I_rI_r}^{(B)} & m_{I_{i+1}I_{i+1}}^{(A)}+c_{i+1}^Ac_{i+1}^Am_{I_rI_r}^{(B)} & & c_{i+1}^Am_{RI_r}^{(B)} \\ \hdashline & & & & & 0 \\ \hdashline 0 & 0 & c_i^Am_{RI_r}^{(B)T} & c_{i+1}^Am_{RI_r}^{(B)T} & 0 & m_{RR}^{(B)} \end{array}\right]\left\{\begin{array}{c} \ddot{\xi}_R^{(A)} \\ \hdashline \vdots \\ \hdashline \ddot{\xi}_{I_i}^{(A)} \\ \hdashline \ddot{\xi}_{I_{i+1}}^{(A)} \\ \hdashline \vdots \\ \hdashline \ddot{\xi}_R^{(B)} \end{array}\right\}$$

$$+\left[\begin{array}{c:c:c:c:c:c} k_{RR}^{(A)} & & k_{RI_i}^{(A)} & k_{RI_{i+1}}^{(A)} & & 0 \\ \hdashline & & & & & 0 \\ \hdashline k_{RI_i}^{(A)T} & & k_{I_iI_i}^{(A)}+c_i^Ac_i^Ak_{I_rI_r}^{(B)} & k_{I_iI_{i+1}}^{(A)}+c_i^Ac_{i+1}^Ak_{I_rI_r}^{(B)} & & c_i^Ak_{RI_r}^{(B)} \\ \hdashline k_{RI_{i+1}}^{(A)T} & & k_{I_iI_{i+1}}^{(A)T}+c_i^Ac_{i+1}^Ak_{I_rI_r}^{(B)} & k_{I_{i+1}I_{i+1}}^{(A)}+c_{i+1}^Ac_{i+1}^Ak_{I_rI_r}^{(B)} & & c_{i+1}^Ak_{RI_r}^{(B)} \\ \hdashline & & & & & 0 \\ \hdashline 0 & 0 & c_i^Ak_{RI_r}^{(B)T} & c_{i+1}^Ak_{RI_r}^{(B)T} & 0 & k_{RR}^{(B)} \end{array}\right]\left\{\begin{array}{c} \xi_R^{(A)} \\ \hdashline \vdots \\ \hdashline \xi_{I_i}^{(A)} \\ \hdashline \xi_{I_{i+1}}^{(A)} \\ \hdashline \vdots \\ \hdashline \xi_R^{(B)} \end{array}\right\}=\left\{\begin{array}{c} 0 \\ \hdashline 0 \\ \hdashline 0 \\ \hdashline 0 \\ \hdashline 0 \\ \hdashline \bar{F}_R^{(B)} \end{array}\right\} \tag{13}$$

Because the displacements (l_1 and l_2) and the interface coordinates (I_i and I_{i+1}) adjacent to the roller (I_r) are changed according to the position of the roller, the mass and stiffness matrices have time variable nonlinear properties. By using the improved method, the dynamic analysis of the combined structure with the nonlinearity of the sliding condition can be easily performed. It can be also applied to the complex structure problems with several substructures and guide lines.

Sliding Condition Example

For the validation of the improved method, the dynamic analysis of the three-substructure-model is performed. The substructures are restricted to each other by the sliding conditions as shown in figure 4. The plates have the same material properties used in the first example, and the spring coefficient is $K = 1000 N/m$. The excitation forces applied at node-150 are $F_y = 30 \times \sin(2\pi \times 70 \times t)\,N$ and $F_z = 500 \times \sin(2\pi \times 70 \times t)\,N$.

Newmark beta method is used to calculate the dynamic response. Figure 5 shows the horizontal displacement of node-150, which is composed of the first mode frequency (37Hz) and the excitation frequency (70 Hz). Figure 6 shows the dynamic motions of the entire structure. It is clear that the dynamic response is adequately obtained by using the improved method.

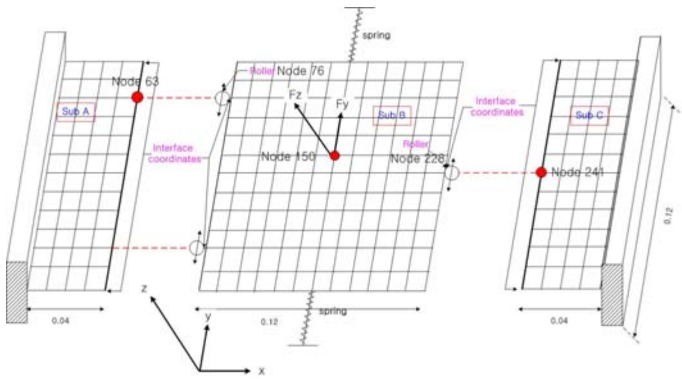

Figure 4 – A scheme of plate model with rollers for dynamic response

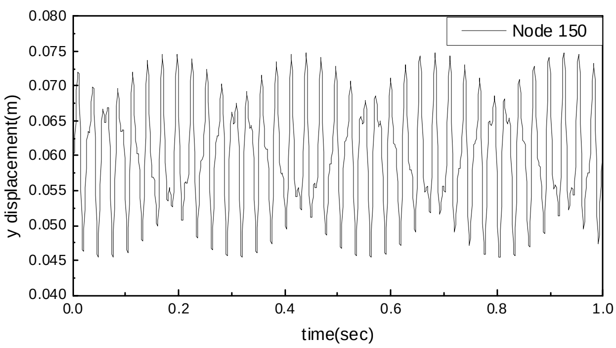

Figure 5 – Dynamic responses of Node 150 for 70Hz excitation.

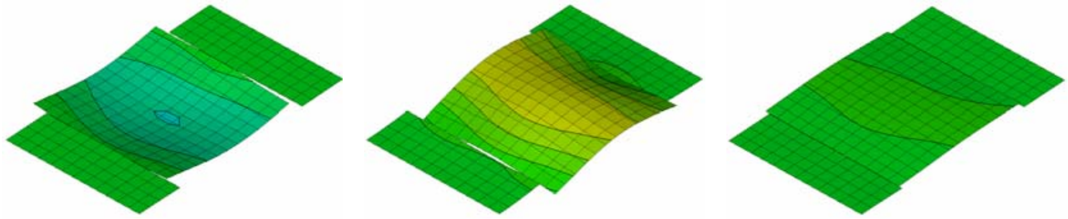

Figure 6 – Dynamic response motions for 70Hz excitation

CONCLUSION

The component mode synthesis method is improved to consider not only the nonlinear hinge but also the sliding mode condition. For the validation of the improved coupling method, a numerical plate model consisting of two substructures and seven torsional springs is synthesized by using the improved method, and then its model parameters are compared with analysis data obtained by NASTRAN®. In order to consider the structural nonlinearity of the sliding mode condition, the improved method is applied to a three-substructure-model with the structural nonlinearity of sliding lines between the substructures, and the coupled structural model is verified with dynamic results. The analysis results show that the improved coupling method is adequate for the structural nonlinear analyses such as the nonlinear hinge and sliding mode condition.

ACKNOWLEDGMENT

This research was supported by the Korea Railroad Research Institute (KRRI) and Yujin Machinery Ltd. This support is gratefully acknowledged.

REFERENCES

[1] Bae, J.S., Kim, D.K., Shin, W.H., Lee, I., and Kim, S.H., "Nonlinear Aeroelastic Analysis of a Deployable Missile Control Fin," *Journal of Spacecraft and Rockets*, Vol. **41**, No. 2, 2004, pp. 264-271.

[2] Craig, R. and Bampton, M, "Coupling of Structures for Dynamic Analyses," *AIAA Journal*, Vol. **6**, 1965, pp. 678-685.

[3] Hunn, B.A., "A Method of Calculating the Normal Modes of an Aircraft," *Quarterly Journal of Mechanics*, Vol. **8**, 1955, pp. 38-58.

[4] Hurty, W.C., "Dynamic Analysis of Structural Systems Using Component Modes," *AIAA Journal*, Vol. **3**, 1965, pp. 678-685.

[5] Karpel, M., and Raveh, D.M, "Fictitious Mass Element in Structure Dynamics," *AIAA Journal*, Vol. **34**, No. 3, 1996, pp. 607-613.

[6] Kim, D.K., Bae, J.S., Lee, I., and Han, J.H., "Dynamic Characteristics and Model Establishment of Deployable Missile Control Fin with Nonlinear Hinge," *Journal of Spacecraft and Rockets*, Vol. **42**, No. 1, 2005, pp. 66-77.